Development of the Generation 3 Particle Pilot Plant Falling Particle Receiver

Brantley Mills[1], Jae Bok Lee[1], Nathan Schroeder[1], Daniel Ray[1], Hendrik F. Laubscher[1], Jeremy Sment[1], Kevin J. Albrecht[1], and Clifford K. Ho[1]

[1] Sandia National Laboratories, Albuquerque, NM, USA

Abstract. A falling particle receiver (FPR) has been designed to integrate with the G3P3-USA pilot plant currently being constructed at the National Solar Thermal Test Facility (NSTTF) at Sandia National Laboratories. This receiver integrates several innovative design features including a converging tunnel (SNOUT), an optimized cavity geometry, and a multistage "catch-and-release" trough. Details about the integration of these features and the final G3P3-USA FPR design and construction are described. Ray-tracing models of the FPR utilizing the NSTTF heliostat field are developed leveraging previous modeling efforts using SolTrace. Models demonstrate that at least 1.5 MW_{th} of incident radiative energy can be provided to the FPR on a clear day throughout a typical year in Albuquerque, NM. Spillage fluxes around the periphery of the aperture are within acceptable bounds for the majority of the year. Intercept factors are computed for each utilized heliostat at the Vernal equinox to provide guidance to heliostat operators during operation of the system.

Keywords: Concentrating Solar Power, Particles, Falling Particle Receiver, Multistage, Ray-Tracing, G3P3

1. Introduction

Falling particle receivers (FPRs) are a promising design for the receiver of a next-generation, particle-based CSP facility supporting electricity generation [1, 2]. Advantages of FPRs include the ability to directly irradiate the particle medium (as the heat transfer fluid), experimental evidence demonstrating average particle outlet temperatures exceeding 800°C [3], low parasitics for particle control, and overall simplicity in the design. FPRs have been experimentally and numerically researched for years at Sandia National Laboratories (SNL) with future pilot scale systems expected to exceed thermal efficiencies of 85% [4]. Recent technoeconomic analyses have also shown that particle-based, utility-scale CSP systems utilizing FPRs may achieve a levelized-cost of electricity (LCOE) of <0.06 $/kWh [5].

The Generation 3 Particle Pilot Plant (G3P3-USA) is a next-generation, particle-based CSP facility [6] currently under construction at the National Solar Thermal Test Facility (NSTTF) at SNL. The purpose of this system is to integrate and demonstrate many of the particle technologies necessary to enable a particle-based CSP facility. A successful demonstration of G3P3-USA will help advance the use of particle-based technologies to meet the 2030 LCOE targets proposed by the Solar Energy Technologies Office within the DOE of < 0.05 $/kWh [7]. The G3P3-USA system features a FPR designed to deliver >1 MW_{th} of heated particles with an average particle temperature exceeding 775°C to the system. Prototype FPRs have been constructed and tested at the NSTTF for years; however, limitations in the experimental setups have prevented continuous on-sun operation for long durations and integration with other critical particle-based infrastructure (which G3P3-USA will address).

After several years of development, the final G3P3-USA FPR design has been completed. The G3P3-USA FPR leverages years of experience gained from testing prototype FPRs at SNL [3, 8-10], a large body of existing literature on FPR technology [11-13], and recent R&D efforts focused on increasing the FPR thermal performance and resilience to operating and environmental conditions (e.g. wind) [4, 6, 14-18]. Specifically, a number of different receiver enhancements have been investigated including: hoods/tunnels around the aperture [14], quartz-half shell aperture covers [15, 18], novel curtain release patterns [19, 20], active air flow over the aperture [16], geometric cavity optimization [14], and multistage features [17]. Of these features, a hood/tunnel (referred to as a solar nod optimized unobstructing tunnel or SNOUT) coupled with an optimized receiver cavity and multistage features were down-selected for integration into the final G3P3-USA design [2].

The purpose of this paper is to highlight how these key design features are integrated into the actual receiver construction while still leveraging the past experience from previous FPR prototypes and testing. This paper highlights construction details of the FPR including the receiver cavity, bottom hopper, feed hopper, receiver slide gate, and SNOUT. In addition, supporting ray-tracing simulations of the G3P3-USA FPR coupled with the NSTTF heliostat field are also presented to define anticipated conditions in Albuquerque, NM throughout a typical year. The remainder of this paper is as follows. First, the G3P3-USA tower is described including the operating conditions and requirements for the FPR. Next, descriptions of the FPR design are provided including details about the subcomponents comprising the FPR system. Then, ray-tracing simulations of the FPR coupled with the NSTTF heliostat field are described and the results are presented. Finally, the conclusions of this paper are summarized.

2. Generation 3 Particle Pilot Plant (G3P3-USA)

The G3P3-USA system [6] is a particle-based 1 MW_{th} CSP pilot plant featuring all necessary components for electricity generation with the exception of the turbomachinery. The G3P3-USA system is being constructed at the NSSTF and utilizes the existing 6 MW_{th} NSTTF heliostat field. However, the presence of the existing NSTTF solar tower necessitates that G3P3-USA is positioned approximately 40 m west and 8 m north of the existing tower center. G3P3-USA is also clocked 21.2° from north facing the centroid of the heliostat field. The location of the tower relative to the field is depicted in Figure 1 with depictions the major components.
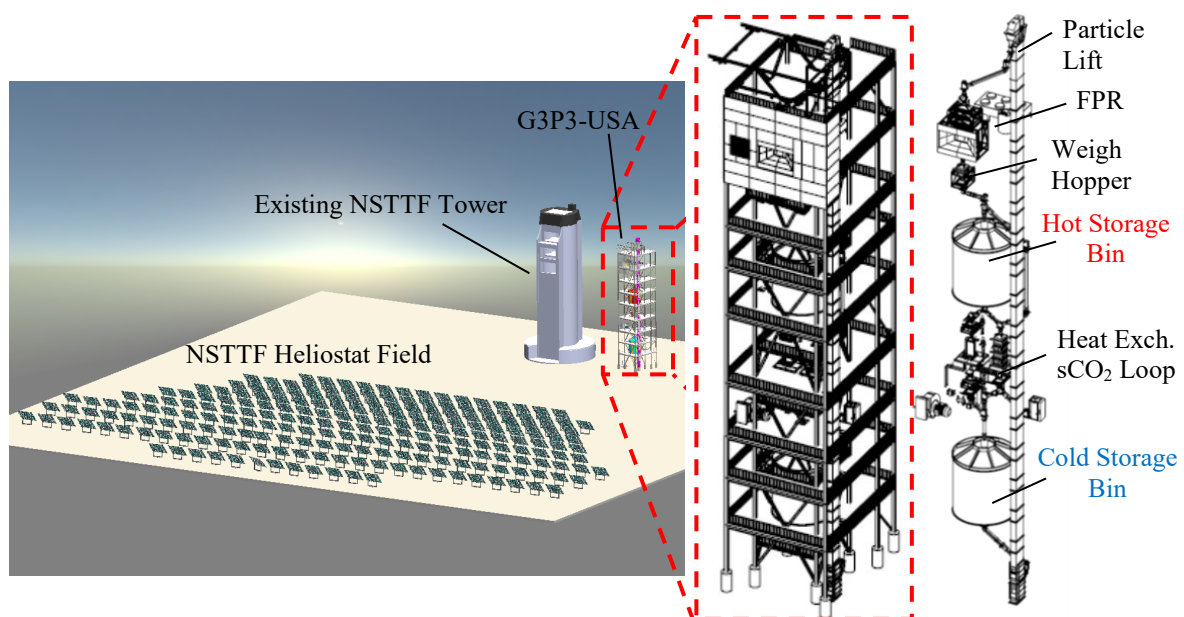

Figure 1. Depiction of the G3P3-USA tower with respect to the NSTTF heliostat field (left) and the G3P3-USA tower and particle loop highlight key components (right).

In brief, G3P3-USA utilizes a FPR that delivers particles at an average outlet temperature exceeding 775°C to a hot storage bin. The FPR is also designed to deliver >6 MW$_{th}$-h of hot particles at the requisite temperature enabling demonstration of energy generation off-sun from thermal energy storage. A weigh hopper immediately below the FPR measures the particle mass flow rate gravimetrically in batches before reaching the hot storage bin (details about the weigh hopper are not included in this paper for brevity). Hot particles leaving the storage bin then travel to a shell-and-plate, particle-to-sCO$_2$ heat exchanger where energy is transferred to the sCO$_2$. Readers are referred to [6] for more details about the storage bins, heat exchanger, and sCO$_2$ loop. Particles exit the heat exchanger and are then stored in a cold storage bin until recirculated to the top of the tower using a bucket lift. The average particle temperature returning to the FPR is expected to be between 550°C and 615°C during normal operation depending on the thermal losses from the system.

3. G3P3-USA Falling Particle Receiver

The G3P3-USA FPR, depicted in Figure 2, consists of three primary components: the receiver cavity, the feed hoper system, and the SNOUT. The design of the receiver cavity and feed hopper borrow many of the lessons learned from testing and maintenance of previous FPR prototypes at the NSTTF. As discussed in the introduction, the SNOUT is a new FPR subsystem that helps improve the thermal performance and resilience of the system in all operating conditions but has not been tested on-sun.
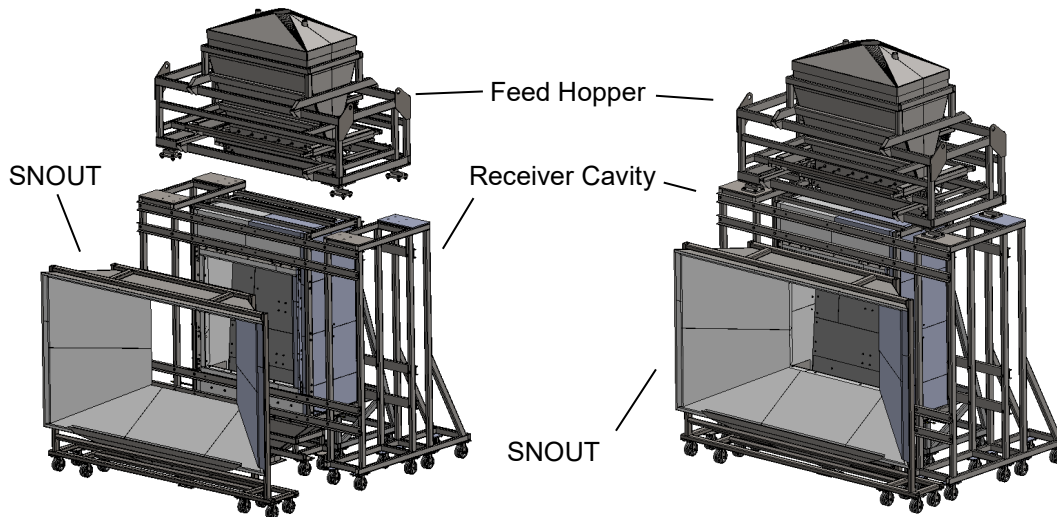
Figure 2. Depiction of the G3P3-USA FPR components.

The FPR is designed for nominal incident radiative powers between 1.5–2 MW$_{th}$ provided from the NSTTF heliostat field. At this nominal incident power, computational models using CFD coupled with discrete ordinates radiation models predict an annualized receiver thermal efficiency $\eta_{th,ann}$ of 83.6% [6]. The thermal efficiency η_{th} is defined as the fraction of radiative energy entering the receiver aperture that is transferred to the particles:

$$\eta_{th} = \frac{Q_{abs}}{Q_{in}} = \frac{\dot{m}\left(h_{out} - h_{in}\right)}{Q_{in}} = \frac{\dot{m}\int_{T_{in}}^{T_{out}} c_P\left(T\right)dT}{Q_{in}} \tag{1}$$

where Q_{abs} is the absorbed thermal power in the particles, Q_{in} is the incident radiative power entering the cavity, $\dot{m}$ is the particle mass flow rate, h is the particle enthalpy, and $c_P(T)$ is the particle specific heat as a function of the *average* particle temperature, T which is defined as:

$$c_P(T) = 388.4 \cdot T^{0.1523} \tag{2}$$

where the fit for the specific heat is derived from Georgia Tech's Thermophysical Properties Database [21]. While the annualized G3P3-USA FPR thermal efficiency is expected to be 83.6%, under certain wind conditions it may be significantly lower particularly at the lowest incident powers where the fraction of advective losses makes a higher percentage of overall thermal energy lost from the system [4]. Rearranging Eq. (1) and substituting in Eq. (2), the following equation for the expected operating linear mass flow rate $\dot{m}/W$ can be derived as:

$$\dot{m}/W = \eta_{th} Q_{in} / \left[\frac{388.4}{1.1523} \left(T_{out}^{1.1523} - T_{in}^{1.1523} \right) W \right] . \tag{3}$$

Note that this calculation assumes that a fixed value of η_{th} is known a priori (for more advanced calculations of η_{th}, the reader is referred to [6]). Eq. (3) is then plotted in Figure 3 for a particle outlet temperature of 800°C, a particle inlet temperature between 550–615°C, and three values of η_{th} with varying incident radiative power. This plot defines an operational particle mass flow rate necessary to deliver the requisite average particle outlet temperature to the system throughout a typical day. As with previous FPR systems developed at the NSTTF [6, 9], this system uses a PID controlled slide gate to control the particle mass flow rate passing through the FPR according to the instantaneous average particle temperature measured in 7 specially design particle collection funnels at the bottom of the cavity (right of Figure 3). This system responds agnostically to any change in efficiency (e.g. from wind) or incident radiative power (e.g. clouds, change in DNI) to deliver the requisite particle outlet temperature within the operational envelope.
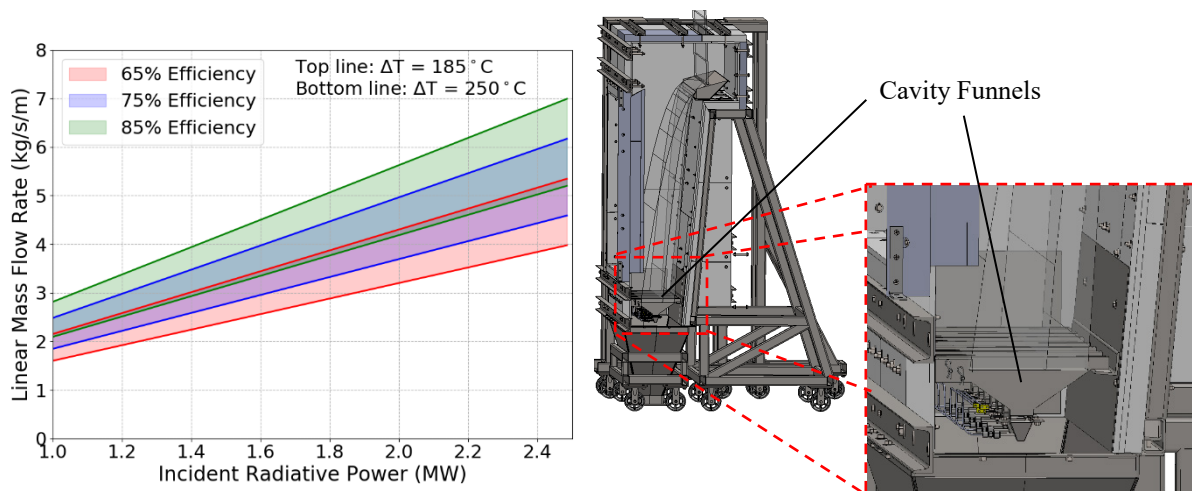

Figure 3. Plot of the linear mass flow rate for the G3P3 FPR at varying η_{th} and Q_{in} to maintain a $185 \leq \Delta T \leq 250°C$ and $T_{out} = 800°C$ (left) and a cutaway of the cavity showing the specially designed particle funnels to instantaneously measure particle outlet temperature (right). A translucent particle curtain envelope is depicted highlighting the expected trajectory.

The FPR cavity is a modular design with a focus on rapid access to the interior for maintenance. The cavity is mounted on grooved casters along rails, and the rear wall of the cavity is separately mounted on an independent frame for access as depicted in Figure 4a. This access also removes logistical constraints where the cavity may be defined as a confined space complicating routine maintenance. Cavity walls are comprised of 2" thick Duraboard® HD and ½" thick RSLE-57 silica composite board (the back wall is 1.5" Duraboard® HD and 1" thick RSLE-57). RSLE-57, as the first-wall material, has demonstrated high survivability in cycling on-sun in previous testing, and both materials exhibit low thermal conductivity and thermal expansion at temperatures of 1000°C. Both insulative layers are overlayed to create more tortuous paths

for hot air to escape the cavity during operation and ceramic fiber sheet is used for further sealing between the outer insulation boards. The boards are bolted to a steel frame, and the bolt ends exposed to the direct irradiation are covered with RSLE-57 pucks that are tapped to screw onto the bolt end (not depicted).
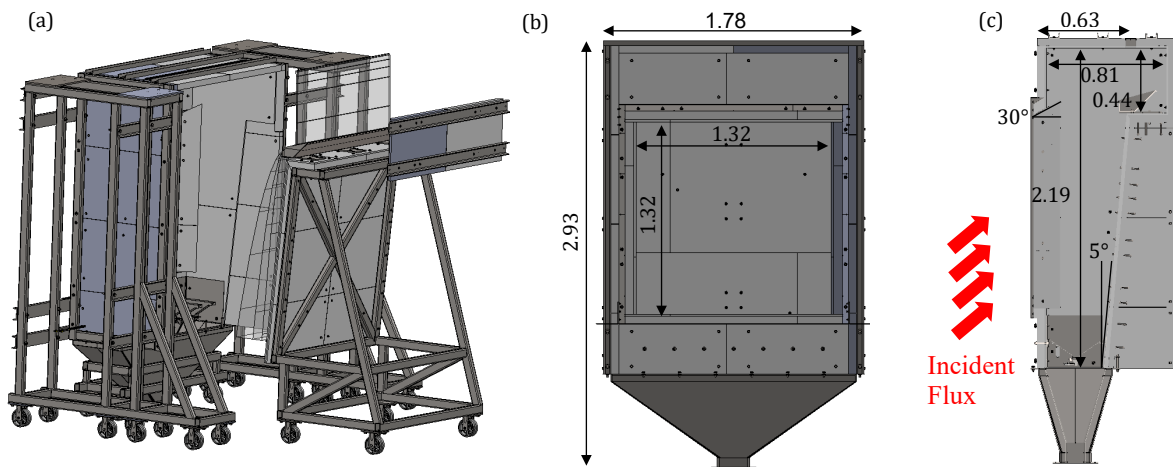

Figure 4. Depiction of the back wall rolled away from the cavity for maintenance (a), front cavity dimensions (b), and side cavity dimensions (c). Dimensions are in meters.

As shown in Figure 4b, a square cavity aperture with dimensions of 1.32 m is selected to simplify construction, and the interior top and side aperture edges are beveled 30° to minimize the normal irradiance on these high flux surfaces. The back wall similarly leans 5° away from vertical to minimize the normal irradiance on the surface while not obstructing the falling particle curtain. The cavity shape and dimensions are primarily informed from geometric optimization studies performed early in the G3P3 development to minimize advective losses from the cavity [14]. A single "catch-and-release" multistage trough (StAIR) [17] is mounted on the back wall 0.44 m below the top cavity surface to slow the particle descent near the peak irradiance. Particles accumulate in the trough and spill over the leading edge shielding any exposed metal surfaces from the concentrated sunlight. By resetting the particle fall velocity, this increases the curtain opacity and protects the cavity back wall [6]. The trough location is determined from cold-flow test measurements using identical troughs in the existing NSTTF FPR [22], but the trough is mounted on translating plates to adjust the location as needed at temperature. Finally, a double-walled stainless steel 304 bottom hopper is located below the cavity. The hopper is internally insulated using >2" thick Microtherm ® Panel-1000R, and the internal lining rests freely on the insulation to accommodate thermal expansion of the steel.

The SNOUT, shown in Figure 5a, consists of a rectangular converging tunnel leading from the spillage board on the "north" G3P3 tower surface to the cavity aperture. The SNOUT is constructed using the same layered insulative board as the cavity bolted to a steel frame on grooved castors. A SNOUT chute is located at the leading edge of the tunnel to re-capture larger particles escaping from the cavity and funnels them to a bypass line near the receiver. The feed hopper, shown in Figure 5b, consists of two distinct systems: a hopper and a slide gate assembly to control the particles entering the cavity. The feed hopper is a double-walled stainless steel 304 wedge hopper with 1.5" thick Microtherm® Panel-1000R insulation internally and a slope of 20°. The hopper was designed to hold a particle inventory of 1800 kg supporting at least 3 minutes of continuous operation at 10 kg/s without refilling. This inventory was necessary to provide a sufficient buffer to accommodate long delivery times provided by the particle bucket lift which operates at a constant speed. Changes to the feed hopper fill rate are not realized until ~3 minutes after a change is made. The receiver slide gate assembly is shown in Figure 5c and Figure 5d. A linear actuator controls the slot width created below the feed hopper based on feedback from the particle outlet temperature and a PID controller. This sys-

tem has been successfully operated at the NSTTF on previous receivers [6, 9]. Additional design changes include the use of a steel enclosure around the gate to maintain more uniform temperatures during operation. The slide gate is suspended within this enclosure using slide gate hangers that also facilitate thermal expansion along the length. Furthermore, the slide gate is ribbed to lower the weight while resisting thermal creep over time at temperatures approaching 615°C.
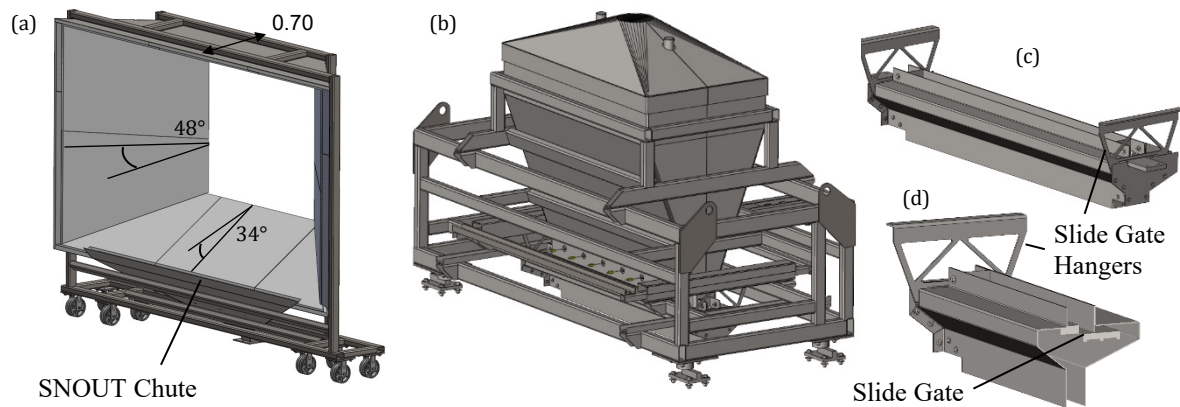

Figure 5. Solid models of the SNOUT (a), feed hopper (b), slide gate assembly (c), and slide gate assembly cut at the midplane (d). Dimensions are in meters.

4. Ray-Tracing Study

As shown in Figure 1, the off-center location of the G3P3-USA tower with respect to the NSTTF heliostat field presents unique challenges in accurately estimating the incident flux on the cavity and surrounding surfaces. Selection of the appropriate heliostats to minimize spillage while maximizing the concentration ratio is important to the overall FPR performance and its survivability. Excessive spillage on the aperture periphery can damage the receiver necessitating downtime for repairs. Therefore, a ray-tracing study is described in this section to predict incident spillage fluxes around the periphery of the aperture, ensure adequate power is available throughout the year, and identify heliostats that are not ideal for use with the G3P3-USA tower. This analysis builds off of previous ray-tracing studies leveraging pre-existing calibrations for the NSTTF heliostat field [4, 18] but using the latest FPR dimensions and location.

The CSP ray-tracing software from NREL, SolTrace [23] (v3.0.0), is utilized in this study. A visualization of the ray-tracing results using this code is shown in Figure 6. The aperture, SNOUT surfaces, and spillage board from the G3P3-USA FPR are included. Key parameters used in the SolTrace model are summarized in Table 1.
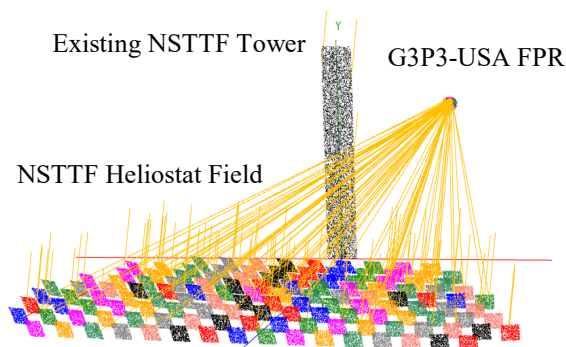
Figure 6. Visualization from ray-tracing simulations of the NSTTF heliostat field with the G3P3-USA FPR (left)

Table 1. SolTrace parameters used in the ray-tracing model.

Parameter	Value
Helio. size	6.1 m x 6.1 m
Helio. reflectivity	0.885
Slope error	1.2 mrad
Specularity error	0.05 mrad
Error type	Gaussian
RSLE reflectivity	0.80
Sun shape	User-defined [4]
Optical errors	Selected
Location	Albuquerque, NM

6

First, the model is executed to ensure that adequate radiative power can be delivered to the aperture throughout a typical year at the NSTTF within ±3 hours of solar noon. The G3P3-USA FPR targets 2 MW$_{th}$ at nominal conditions, but at least 1.5 MW$_{th}$ is desired further from solar noon. Heliostats in the NSTTF field are iteratively selected to maximize the power reaching the aperture while minimizing the spillage fluxes. TMY2 data for Albuquerque, NM, USA is leveraged to determine appropriate DNI values on a clear day at the winter and summer solstices and the equinox. The results of the study are summarized in Table 2 and the number of ray intersections was selected such that error in the peak flux was <1%.

Table 2. Incident radiative fluxes on the G3P3-FPR throughout a typical year in Albuquerque, NM. Aperture columns define the fluxes entering the cavity and SNOUT/Spillage Board columns define the peak spillage fluxes around the receiver (>650 kW/m^2 are highlighted).

Season	Time (hr)	DNI (W/m^2)	Aperture			SNOUT (east)	SNOUT (west)	Spillage Boards
			Peak flux (MW/m^2)	Avg. flux (MW/m^2)	Q_{in} (MW)	Peak flux (kW/m^2)	Peak flux (kW/m^2)	Peak flux (kW/m^2)
Vernal Equinox	-3	850	1.5431	0.93648	1.6033	624.2	574.5	593.3
	Noon	950	1.9418	1.1166	1.9116	566.5	559.1	598.9
	+3	850	1.7	1.0153	1.7381	591.44	519.1	419.1
Summer Solstice	-3	900	1.3013	0.8946	1.5316	587.22	467.51	**665.41**
	Noon	950	1.5876	1.015	1.7377	576.97	457.46	631.89
	+3	900	1.6461	1.0799	1.8487	**655.31**	585.88	522.69
Winter Solstice	-3	700	1.4907	0.89132	1.5259	**664.23**	588.06	305.38
	Noon	950	2.0376	1.1605	1.9868	648.36	620.32	515.56
	+3	700	1.7911	1.0949	1.8745	645.82	558.99	474.72

As seen in Table 2, the radiative power delivered to the aperture Q_{in} exceeds 1.53 MW$_{th}$ throughout the year on a typical clear day. Recall that each defined time may use a different number of heliostats depending on the conditions for that time (determined iteratively). Using a constant annualized FPR thermal efficiency of 83.6%, the total thermal energy delivered to the particles over 6 hours centered around solar noon can be estimated on each day by integrating under the curve defined by the three points in Table 2. At the equinox, summer solstice, and winter solstice, the thermal energy transferred to the particles is 9.42, 8.60, and 9.53 MW$_{th}$-h, respectively.

Peak spillage fluxes around the receiver throughout the year are also defined in Table 2. Previous simulation results in quiescent conditions [4] have shown that peak temperatures on the periphery of the aperture using a SNOUT can be estimated from the peak spillage fluxes. Fluxes between 600–700 kW/m^2 translate to peak temperatures between 1239–1450°C (where the absence of wind likely adds to the conservatism of this estimate). As shown, peak fluxes were simulated to reach 655 kW/m^2 which exceeds maximum temperature limits of ~1200°C for RSLE-57. This suggests that lower powers may be necessary at certain times throughout the year. Peak fluxes on the spillage boards (<655 kW/m^2) with a large viewfactor to the ambient environment are well below maximum limits of <1000–2000 kW/m^2 determined experimentally from testing [10].

Finally, the ray-tracing model is leveraged to identify the best heliostats for the unique location of the G3P3-USA tower. An intercept factor (IF) is computed for each heliostat in the NSTTF heliostat field utilized at solar noon on the Vernal equinox. The IF is defined as the fraction of reflected light that reaches the G3P3-USA FPR aperture. The results are plotted in Figure 7a. The corresponding incident solar flux on the aperture is shown in Figure 7b. As shown in the Figure 7a, eastern heliostats on the front two rows of the NSTTF heliostat field have very low IF <0.25 suggesting that they are suitable candidates to exclude to minimize

flux on the western surfaces of the SNOUT. Heliostats with high IF will be prioritized in G3P3 testing to minimize spillage while increasing the overall power delivered to the receiver.
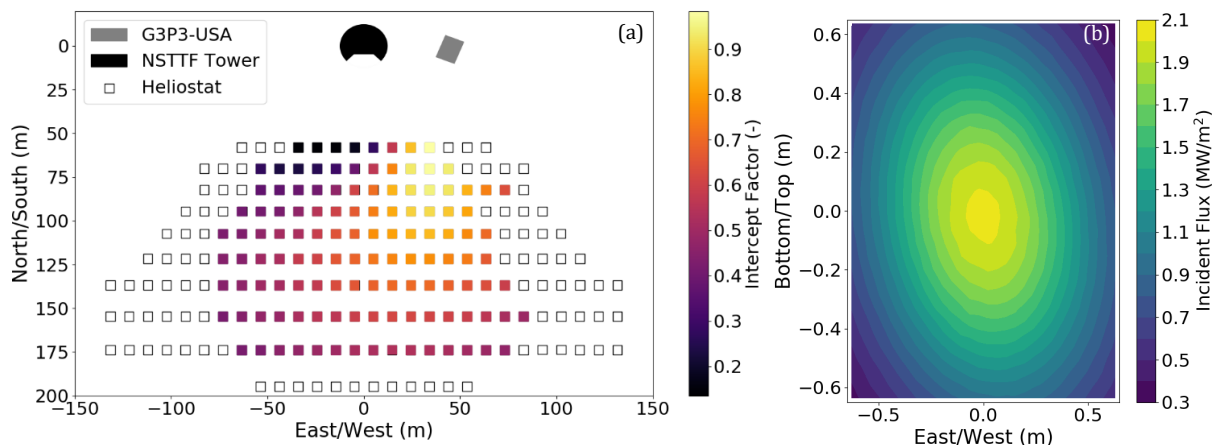
Figure 7. Plot of the NSTTF heliostat intercept factors for the heliostats utilized at solar noon on the Vernal equinox. Uncolored heliostats are not utilized. (a) Corresponding incident solar flux on the aperture (b)

5. Conclusions

The Generation 3 Particle Pilot Plant (G3P3-USA) is a next-generation, particle-based CSP facility currently under construction at the National Solar Thermal Test Facility (NSTTF) at Sandia National Laboratories. The purpose of this system is to integrate and demonstrate many of the particle technologies necessary to enable a particle-based CSP facility. The system features a falling particle receiver (FPR) designed to heat particles up to temperatures exceeding 775°C. The final G3P3-USA FPR design has been completed and critical details about the design and construction have been discussed. The integration of several critical design features including the SNOUT, multistage "catch-and-release" troughs, and a PID controlled slide gate have been highlighted.

Ray-tracing models of the G3P3-USA tower utilizing the NSTTF heliostat field have been developed in SolTrace. The models were exercised to show that > 1.5 MW_{th} could be provided to the FPR aperture within ±3 hours of solar noon throughout the year. Spillage fluxes around the periphery of the aperture were shown to be <665 kW/m^2. In total, between 8.60 and 9.53 MW_{th}-h of thermal energy can be provided to the particles throughout the year on a clear day. Intercept factors to each heliostat were computed for solar noon at the Vernal equinox to provide guidance to heliostat operators on the ideal heliostats to utilize during operation.

Data availability statement

The data that support the findings of this study are available from the lead author, Brantley Mills, upon reasonable request and approval of Sandia National Laboratories.

Author contributions

Brantley Mills: Conceptualization, Methodology, Visualization, Writing – original draft Jae Bok Lee: Formal Analysis, Investigation, Visualization Nathan Schroeder: Conceptualization Daniel Ray: Conceptualization Hendrick F. Laubscher: Conceptualization Jeremy Sment: Conceptualization, Project administration Kevin J. Albrecht: Conceptualization Clifford K. Ho: Conceptualization, Project administration

Competing interests

The authors declare no competing interests.

Funding

Acknowledgement

References

1. Ho, C.K., 2016, "A review of high-temperature particle receivers for concentrating solar power", Applied Thermal Engineering, 109, pp. 958-969, B. DOI: 10.1016/j.applthermaleng.2016.04.103
2. Mills, B.H., Ho, C.K., Schroeder, N.R., Shaeffer, R., Laubscher, H.F., Albrecht, K.J., 2022, "Design Evaluation of a Next-Generation High-Temperature Particle Receiver for Concentrating Solar Thermal Applications", Energies, 15(5), p. 1657. DOI: 10.3390/en15051657
3. Ho, C.K., Schroeder, N.R., Labuscher, H.L., Yue, L., Mills, B., Shaeffer, R., Christian, J.M., Albrecht, K.J., 2020,"Receiver Design and On-Sun Testing for G3P3-USA", SolarPACES 2020, Virtual Online Conference.
4. Mills, B., Shaeffer, R., Yue, L., Ho, C.K., 2020, "Improving Next-Generation Falling Particle Receiver Designs Subject to Anticipated Operating Conditions", ASME 2020 14th International Conference on Energy Sustainability, Virtual Online Conference, June 17–18. DOI: 10.1115/ES2020-1667
5. González-Portillo, L.F., Albrecht, K.J., Ho, C.K., 2021, "Techno-economic optimization of CSP plants with free-falling particle receivers", Entropy, 23(1), p. 76. DOI: 10.3390/e23010076
6. Ho, C.K., Sment, J., Albrecht, K.J., Mills, B., Schroeder, N., Laubscher, H., González-Portillo, L.F., Libby, C., Pye, J., Gan, P.G., Wang, Y., 2021,"Gen 3 Particle Pilot Plant (G3P3) – High-Temperature Particle System for Concentrating Solar Power (Phases 1 and 2)", Sandia National Laboratories, pp. 1-212.
7. 2030 Solar Cost Targets, 2021. https://www.energy.gov/eere/solar/articles/2030-solar-cost-targets. (Accessed December 13, 2021).
8. Ho, C.K., Christian, J.M., Yellowhair, J., Siegel, N., Jeter, S., Golob, M., Abdel-Khalik, S.I., Nguyen, C., Al-Ansary, H., 2016, "On-sun testing of an advanced falling particle reciever system", AIP Conference Proceedings, 1734, p. 030022 (8 pages). DOI: 10.1063/1.4949074

9. Ho, C.K., Peacock, G., Christian, J.M., Albrecht, K.J., Yellowhair, J.E., Ray, D., 2019, "On-Sun Testing of a 1 MW$_t$ Particle Receiver with Automated Particle Mass-Flow and Temperature Control", AIP Conference Proceedings, 2126(1), p. 030027 (9 pages). DOI: 10.1063/1.5117539

10. Christian, J., Ho, C.K., 2016, "Design requirements, challenges, and solutions for high-temperature falling particle receivers", AIP Conference Proceedings, 1734, p. 030008 (8 pages). DOI: 10.1063/1.4949060

11. Kim, J.-S., Kumar, A., Gardner, W., Lipiński, W., 2019, "Numerical and Experimental Investigation of a Novel Multi-Stage Falling Particle Receiver", AIP Conference Proceedings, 2126(1), p. 030030 (8 pages). DOI: 10.1063/1.5117542

12. Kim, J.-S., Gardner, W., Potter, D., Too, Y.C.S., 2020, "Design of a multi-stage falling particle receiver with truncated-cone", AIP Conference Proceedings, 2303(1), p. 030023 (7 pages). DOI: 10.1063/5.0029524

13. Gobereit, B., Amsbeck, L., Buck, R., Pitz-Paal, R., Röger, M., Müller-Seinhagen, H., 2015, "Assessment of a falling solid particle receiver with numerical simulation", Solar Energy, 115, pp. 505-517. DOI: 10.1016/j.solener.2015.03.01

14. Mills, B., Schroeder, B., Yue, L., Shaeffer, R., Ho, C.K., 2019, "Optimizing a Falling Particle Receiver Geometry Using CFD Simulations to Maximize the Thermal Efficiency", AIP Conference Proceedings, 2303(1), p. 030027 (11 pages). DOI: 10.1063/5.0029331

15. Yue, L., Mills, B., Christian, J., Ho, C.K., 2021, "Effect of quartz aperture covers on the fluid dynamics and thermal efficiency of falling particle receivers", Journal of Solar Energy Engineering, 144(4), p. 041008 (13 pages). DOI: 10.1115/1.4053449

16. Yue, L., Shaeffer, R., Mills, B., Ho, C.K., 2019, "Active Airflow for Reducing Advective and Particle Loss in Falling Particle Receivers", AIP Conference Proceedings, 2303(1), p. 030036 (11 pages). DOI: 10.1063/5.0031223

17. Yue, L., Schroeder, N., Ho, C.K., 2020, "Particle Flow Testing of a Multistage Falling Particle Receiver Concept: Staggered Angle Iron Receiver (StAIR)", ASME 2020 14th International Conference on Energy Sustainability, Virtual Online Conference, June 17–18. DOI: 10.1115/ES2020-1666

18. Yellowhair, J., Ho, C.K., 2019, "Optical ray-tracing performance modeling of quartz half-shell tubes aperture cover for falling particle receiver", ASME 2019 13th International Conference on Energy Sustainability, Bellevue, WA, USA, July 14–17. DOI: 10.1115/ES2019-3927

19. Ho, C.K., Christian, J.M., Yellowhair, J., Ortega, J., Andraka, C., 2016, "Fractal-Like Receiver Geometries and Features for Increased Light Trapping and Thermal Efficiency", AIP Conference Proceedings, 1734, p. 030021 (8 pages). DOI: 10.1063/1.4949073

20. Mills, B., Ho, C.K., Christian, J.M., Peacock, G., 2017, "Novel Particle Release Patterns for Increased Receiver Thermal Efficiency", AIP Conference Proceedings, 1850(1), p. 030035 (8 pages). DOI: 10.1063/1.4984378

21. Thermophysical Properties Database of Gen3 CSP Materials, 2021. http://gen3csp.gatech.edu/. (Accessed 2020).

22. Schroeder, N., Mills, B., Ho, C.K., 2022, "Characterization of Particle Curtain Forward Translation in Multistage Release Falling Particle Receivers", ASME 2022 16th International Conference on Energy Sustainability, Philadelphia, PA, July 11-13.

23. Wendelin, T., 2003, "SolTRACE: A New Optical Modeling Tool for Concentrating Solar Optics", ASME 2003 International Solar Energy Conference, Kohala Coast, Hawaii, USA, March 15-18. DOI: 10.1115/ISEC2003-44090